

THE EFFECTS OF IMPACT PROCESSING ON THE STABLE ISOTOPE COMPOSITION OF THE MOON. A. M. Gargano^{1,2}, E.J. Cano², K. Ziegler³, Z. Sharp^{2, 4}, C.K. Shearer³, J.M.D. Day¹, and the ANGSA Science Team⁵. ¹Scripps Institution of Oceanography, University of California San Diego, 92093 (amgargano@ucsd.edu), ²Center for Stable Isotopes, University of New Mexico, Albuquerque, 87131, ³Institute of Meteoritics, University of New Mexico, Albuquerque, 87131, ⁴Department of Earth and Planetary Sciences, University of New Mexico, Albuquerque, 87131, ⁵Lunar and Planetary Institute, Houston TX 77058, ⁵Jacob-JETS Contract, NASA Johnson Space Center, Houston, TX, 77058, USA, ⁶ANGSA Science Team

Introduction: The Apollo sample suite contains a wide-breadth of materials from the lunar surface which manifest varying extents of impact processing (e.g., shock-induced volatile-loss), including impactor mixing. The geochemical effects of these processes likely influenced lunar chemistry and occurred in tandem with magmatic evolution of the Moon following the Giant Impact. Although rocks such as impact melt breccias contain clear evidence for impactor contamination [1], crustal lithologies such as anorthosites retain the largest ranges in volatile-element stable isotope compositions (K, Cl, Zn [2, 3, 4]) of lunar materials that are difficult to explain by igneous processes.

Impactor mixing and impact processing could partly explain these compositions. Impactor-derived volatile reservoirs contain far higher initial volatile contents than can be reasonably achieved by igneous processes (e.g., urKREEP), and therefore larger ranges in stable isotope compositions can be achieved by later evaporation/condensation. Further, impact processing throughout magma ocean crystallization could serve to open conduits for volatile outgassing [5] and contribute impactor-derived highly-siderophile elements to the Moon [6, 7]. Here, we aim to provide a better understanding of the extent to which lunar volatiles could be reasonably derived from impactors, and whether impact processing resulted in significant evaporative mass loss.

Impact processing of lunar regolith: Lunar regolith is a logical reservoir of interest for studying the effects of impact processing of the lunar surface. Regolith contains an array of impact processed materials. As a ‘bulk’ material, it represents the breakdown of primary mineral phases to a small grain size (e.g., ‘fines’ <10-20 μm) dominated by glasses, including variably vesicular agglutinates [8, 9]. Micrometeorite impacts which rework the regolith can reach temperatures from ~1700-3800 K – sufficient to cause silicate evaporation [10]. While the major and minor element chemistry of agglutinates (an impact glass) reflects the preferential loss of more volatile mafics (Fe, Mg) and enrichment in plagioclase (Ca, Al)[8, 11, 12], the increased surface area of the finest fraction results in systematic volatile metal enrichments from vapor deposition (e.g., Zn, Pb, Cd)[13]. A dynamic equilibrium exists throughout

impact driven surface processing – serving to both deplete and enrich volatile elements throughout the relatively short residence time of lunar surface regoliths (~ tens of millions of years [14, 15]).

Buffering evaporative mass-loss with impactor addition: Despite clear evidence for vaporization and deposition, regolith does not contain particularly extreme volatile element stable isotope compositions (i.e., only a few ‰ higher in $\delta^{66}\text{Zn}$ and $\delta^{37}\text{Cl}$ values when compared to mare basalts [16, and references therein]) and is volatile-rich relative to most feasible precursor materials. Similarly, the $\delta^{18}\text{O}$ values of regolith are not significantly higher than their protoliths [17]. This suggests that either minimal evaporation occurs during regolith maturation, or conversely, that mass-loss is buffered by meteoritic addition (estimated to be 1-2% [18, 19]). As the isotopic compositions of volatile elements can be overprinted by processes not directly related to impactor flux - we instead utilize high precision triple oxygen isotopes to constrain the subtle contribution of impactor(s) and silicate evaporation during impact processing.

Results: We performed a silicate evaporation experiment – via CO_2 laser heating under vacuum – of a mid-ocean ridge basalt, which yielded a range of $\delta^{18}\text{O}$ values from 5.5 to >20‰ (Fig. 1). We were unable to measure the mass loss from the experiment. However, by extrapolating similar data from [20] – the O isotope enrichments can be estimated to result from up to ~90% mass loss. In $\delta^{18}\text{O}$ vs. $\delta^{17}\text{O}$ space, the slope of silicate evaporation is approximately 0.518, yielding a

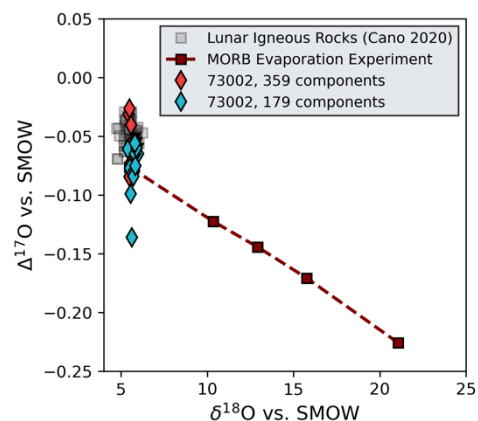


Figure 1: $\delta^{18}\text{O}$ vs $\Delta^{17}\text{O}$ of lunar materials and MORB evaporation experiment.

decrease in the $\Delta^{17}\text{O}$ with increasing $\delta^{18}\text{O}$ values. We also measured the triple oxygen isotope compositions of several impact melt splatters (IMS) and components from mature lunar soils – 73002-172 and 73002-359 ($\text{Is}/\text{FeO} > 50$)(Fig. 2) following methods outlined in [21]. The $\Delta^{17}\text{O}$ values of IMS are generally higher than the bulk-silicate Moon (BSM)($\sim -0.055\text{‰}$), and markedly different from host anorthosite (see ‘X’ in Fig. 2). In contrast, impact glass and bulk regolith are

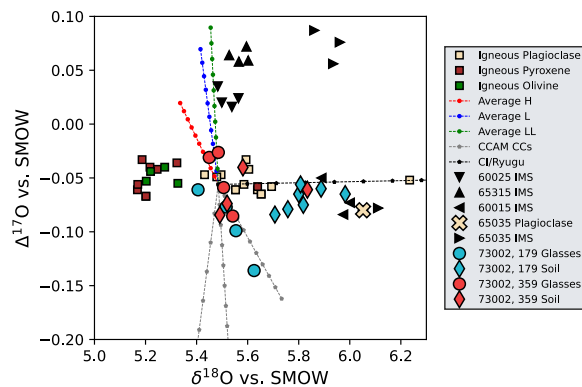


Figure 2: $\delta^{18}\text{O}$ vs $\Delta^{17}\text{O}$ values of lunar materials [25]. Mixing lines depict 1-10% mixtures of OC and CC-like impactors. CC-mixtures are chosen on the CCAM line with $\delta^{18}\text{O}$ values of 4, 6, and 8‰, respectively. CI/Ryugu data from [26]. Remaining lunar data from [21].

generally characterized by negative $\Delta^{17}\text{O}$ values down to -0.15‰ (Fig. 2).

Discussion: Lunar IMS and regolith are generally thought to contain a 1-2% impactor component [18, 19, 21]. While the triple oxygen isotope composition of regolith glasses are consistent with a 1-7% CCAM-derived carbonaceous chondrite-like component, apart from 60015, IMS contain $>5\%$ of ordinary chondrite-like oxygen. These estimates exceed those derived from siderophile element contents, which may reflect the increased importance of vapor phase deposition and/or oxygen diffusion [22]. Indeed, vapor deposits on soil particle rims exhibit oxygen superstoichiometry [23]. Solar wind could also contribute non-lunar oxygen; however, the $\delta^{17}\text{O}$ & $\delta^{18}\text{O}$ values of this potential component are *extremely* low ($< -50\text{‰}$)[24], and therefore is unlikely to be a significant contributor of the measured oxygen.

Instead, the bulk-regolith triple oxygen isotope composition has slightly higher $\delta^{18}\text{O}$ (approximately $+0.5\text{‰}$ [17], and lower $\Delta^{17}\text{O}$ values compared to primary lunar protoliths (e.g., mixtures of olivine, pyroxene & plagioclase [21]). This could be explained by a loss of mafic components – with low $\delta^{18}\text{O}$ values – throughout regolith maturation [11, 12]. This process would serve to increase bulk regolith $\delta^{18}\text{O}$ values and may occur alongside subtle silicate evaporation. How-

ever, this process is not a unique solution as impactor addition of CC/CI-type impactors yields a similar result. These possibilities need to be further refined by impactor-specific isotopic/chemical tracers, such as nucleosynthetic isotope anomalies (e.g., [25]). We will include more detailed mixing models to better constrain the conclusions of this work.

Acknowledgements: Ideas for this work were greatly informed by the ANGSA/Apollo 17 Workshop and discussions with the ANGSA Mission Science team. NASA SSW grant #80NSSC22K0098 supported this work.

References: [1] Puchtel, I. S. et al. (2008) *GCA*, 72(12), 3022-3042. [2] Tian, Z. et al. (2020). *GCA*, 280, 263-280. [3] Kato C. et al. (2015) *Nature communications*, 6, 1-4. [4] Gargano, A. et al. (2020) *PNAS*, 117, 23418-23425. [5] Barnes, J. J. et al. (2016). *Nature communications*, 7(1), 1-10. [6] Day, J. M. D., et al. (2010). *EPSL*, 289, 595-605. [7] Zhu, M. et al. (2019). *Nature*, 571, 226-229. [8] Papike, J. J. et al. (1982). *Reviews of Geophysics*, 20, 761-826. [9] McKay, D. S., & Basu, A. (1983). *Journal of Geophysical Research: Solid Earth*, 88, B193-B199. [10] Cintala, M. J. (1992). *Journal of Geophysical Research: Planets*, 97(E1), 947-973. [11] Devine, J. M. et al. (1982). *Journal of Geophysical Research: Solid Earth*, 87, A260-A268. [12] Warren, P. H., & Korotev, R. L. (2022). *MAPS*, 57(2), 527-557. [13] Krähenbühl, U. (1980) *LPSC*, 11, 1551-1564. [14] Hörz, F. et al. (2020). *Planetary and space science*, 194, 105105. [15] O'Brien, P., & Byrne, S. (2021). *Journal of Geophysical Research: Planets*, 126, e2020JE006634. [16] Gargano, A. et al. (2022). *American Mineralogist*, 107(11), 1985-1994. [17] Clayton, R. N. et al. (1974). *LPSC*. (Vol. 5, pp. 1801-1809). [18] Baedecker, P. A. et al. (1974). *LPSC*, 5, 1625-1643. [19] Morris, R. V. et al. (1986), *Journal of Geophysical Research: Solid Earth*, 91, E21-E42. [20] Young, E. D. et al. (1998), *GCA*, 62(18), 3109-3116. [21] Cano, E. J. (2020). *Nature Geoscience*, 13(4), 270-274. [22] Neuman, M. (2022), *LPI Contributions*, 2704, 2027. [23] Zook, H. A. (1975). *LPSC*, 6, 1653-1672. [24] Keller, L. P. & McKay, D. S. (1997). *GCA*, 61(11), 2331-2341. [25] McKeegan, K. D. (2011). *Science*, 332(6037), 1528-1532. [26] Worsham, E. A. & Kleine, T. (2021). *Science advances*, 7(44), 2837. [27] Greenwood, R. C. (2022). *Nature Astronomy*, 1-10.